Physical and mechanical behavior of hot rolled HDPE/HA composites

A. PANDEY, E. JAN, P. B. ASWATH*
Materials Science and Engineering Program, University of Texas at Arlington, Arlington, TX, 76019, USA

Published online: 12 April 2006

In the present study hydroxyapatite (HA) reinforced high-density polyethylene (HDPE) composites were synthesized with possible application as orthopedic implants. HDPE was reinforced with HA particles using a novel hot rolling technique that facilitated uniform dispersion and blending of the reinforcements in the matrix. Composites were processed with up to 50 wt.% HA particles. Scanning Electron Microscopy studies confirmed uniform particle distribution of the reinforcement. Mechanical properties of the composites were examined by tensile tests. Increasing volume fraction of reinforcement from 10–50 wt.% resulted in a 150% increase in elastic modulus and 20% increase in tensile strength. Differential Scanning Calorimetry, Fourier Transformed Infrared spectroscopy and X-ray Diffraction studies indicate that the new blending process can be used to synthesize a crystalline, uniformly reinforced composite having chemical affinity between the matrix and reinforcement.

1. Introduction

Hydroxyapatite (HA) reinforced high-density polyethylene (HDPE) composite has been under study since early 1980s, when Bonfield *et al*. proposed and lead the pioneering work to develop these kinds of composites as an alternative material for bone replacement [1–8]. Calcium hydroxyapatite (HA) as a ceramic biomaterial has been widely used for biological applications [1–9]. Hydroxyapatite (Ca5 (PO4)3OH), one of the main constituents of natural bone (70 wt.%) [10] is the stable phase of calcium phosphate at body temperature and pH $>$ 4.2 [11]. When implanted, a cascade of physiochemical interactions takes place with the biological environment, resulting in the build up of interfacial layers that bond the bone tissue to the implant material [12–14]. Adsorption of ions and biomolecules, formation of calcium phosphate (apatite) layers, followed by interactions with various cells are the three main processes that occur after implantation [13].

The use of implants for a load bearing application depends on the development of a material having sufficient mechanical strength and biocompatibility. Such bone-matching mechanical performances can be achieved by combining high toughness matrix of a polymer and a bone-like stiff ceramic phase that provides mechanical reinforcement and the bioactive character of the implant. In the present study a high strength HDPE matrix reinforced with ceramic hydroxyapatite particles was developed.

In a simple HA-HDPE system, there exist only two phases: dispersed hydroxyapatite ceramic particles and continuous high-density polyethylene. Various synthesis and designing routes to obtain HA-HDPE biomaterial have been developed. Injection molding and extrusion are most common of these processes that yield material of desired porosity and mechanical characteristic [1, 2, 7–9]. Mechanical properties of HA-HDPE composite that is manufactured via an established conventional route approach the lower bound for human cortical bone [6].

Adhesion of reinforcement to the matrix can have a significant influence on the characteristics and properties of the composites [9]. Polyethylene is a non-polar, hydrophobic polymer, and consequently, only mechanical interlocking exists between the HA particles and the polyethylene matrix in a conventionally processed HA-HDPE composite [6]. A chemical interaction between the filler and the polymer will lead to much improved bonding, and hence mechanical properties [9].

In the present study, we have achieved improved mechanical properties of the HA-HDPE composite, by changing the processing method, leading to better chemical interaction between the filler and the polymer matrix.

*Author to whom all correspondence should be addressed.
0022-2461
DOI: 10.1007/s10853-005-5350-9

Hot rolling cannot replace injection molding or extrusion as shaping method, but it can be a first step in composite preparation followed by final shaping methods for implant fabrication. Characterization of the samples was done using SEM, XRD, DSC and FTIR to examine the presence of chemical coupling between the filler and the polymer matrix.

2. Experimental

2.1. Materials

High Density Polyethylene was purchased from Alfa Aesar. Hydroxyapatite was also obtained from Alfa Aeser (particle size 10–15 micron) and was used as obtained without further purification or processing.

2.2. Composite synthesis

HDPE-HA composites investigated were synthesized by melt blending of HDPE and HA in a 2 roll mill ensuring a uniform distribution of HA in the HDPE matrix. HDPE pellets were introduced between the 2 hot rolls (preheated at 145°C), rolling in opposite directions. A predetermined amount of HA powder was also added (to the rolls). Sufficient number of passes between the rolls was made to ensure complete blending and uniform distribution of filler particles in the polymer matrix. After rolling the composites were hot pressed at 80°C for one hour.0.3 cm thick dumbbell shaped tensile specimens were prepared with a gauge length of 5.08 cm. The composition of the HA reinforced HDPE composites under study are listed in Table I.

2.3. Tensile testing

Mechanical properties of HA-HDPE composites were evaluated by tensile testing. These specimens were subsequently annealed at 60°C and were tested 48 h after the heat treatment. Normal tensile tests were conducted on a MTS Q- Test 150 testing machine at a crosshead speed of 25 mm/min. Extensometer was used to measure specimen extension in order to determine its Young's modulus and strain. The test was continued to the fracture of the specimen. A 10 KN load cell was used for tensile tests. Load-extension curves were recorded. At least five specimens were tested for each composition of the composites.

2.4. SEM and EDX analysis

A scanning electron microscope (JEOL JSM-IC 845 A) was used to examine fracture surfaces of HA-HDPE composites. SEM specimens were cut from fractured composite pieces and mounted onto SEM stubs. Samples were cleaned with compressed air jet and lightly gold coated before examination (approx 400–700 $\times$ 10^{-8} cm thick layer).

TABLE I Composition of HDPE composites investigated

Sample number	wt% Hydroxyapatite
1	10%
2	20%
3	30%
4	40%
5	50%

2.5. FTIR analysis

FTIR spectra of the HA-HDPE composites were recorded on a Bruker VT 30 spectrophotometer. Spectra of the composites were obtained in diffuse reflectance mode. Spectra in the range of 400 cm^{-1} to 4000 cm^{-1} were recorded for 256 scans at 1^{-1} resolution. IR spectrum of HA powder, HDPE pellets, hot rolled HDPE and hot rolled HA-HDPE composite were recorded for comparative evaluation/understanding of various structural interaction.

2.6. XRD analysis

Powder X-ray diffraction spectrum of HA powder, hot rolled HDPE and hot rolled HA-HDPE were recorded on a Siemens D-500 X-ray diffractometer. Measurements were carried out to see if the polymer crystallinity was maintained after hot rolling. Slow scans were run at 0.1° interval and 6 s dwell time.

2.7. DSC analysis

Differential Scanning Calorimetric studies were carried out on a Perkin Elmer TA 7 analyzer. Approx 5 mg of sample was used for all DSC measurements. Temperature scan rate was fixed at 5°C/ min and N_2 environment was maintained in the furnace.

3. Results and discussion

3.1. Distribution of HA in HDPE composites

A uniform distribution of reinforcement particles in a HDPE matrix was observed. *A* low magnifications, SEM pictures clearly showed that the filler particles were uniformly distributed and no agglomeration of HA particles could be observed. Use of coupling agents for uniform distribution of filler particles has been proposed in earlier studies [15, 16] for extruded particle reinforced composites where agglomeration and porosity was an issue, but no such problem were encountered in the present study. Figure 1a–e shows SEM images of the composite specimens at a magnification of 500, showing no agglomeration, uniform distribution and absence of voids without the use of any chemical modifier.

Study of the fracture surface shows that hydroxyapatite particles are firmly held by the polymer matrix and during tension testing these particles are pulled out of the polymer matrix. Fig. 2 shows a typical fracture surface at a magnification of 4500. Hydroxyapatite particles are pulled out of the polymer matrix due to strain mismatch between a ceramic hydroxyapatite particles and highly ductile polymer matrix. Examination of these hydroxyapatite particle at even higher magnification revealed that

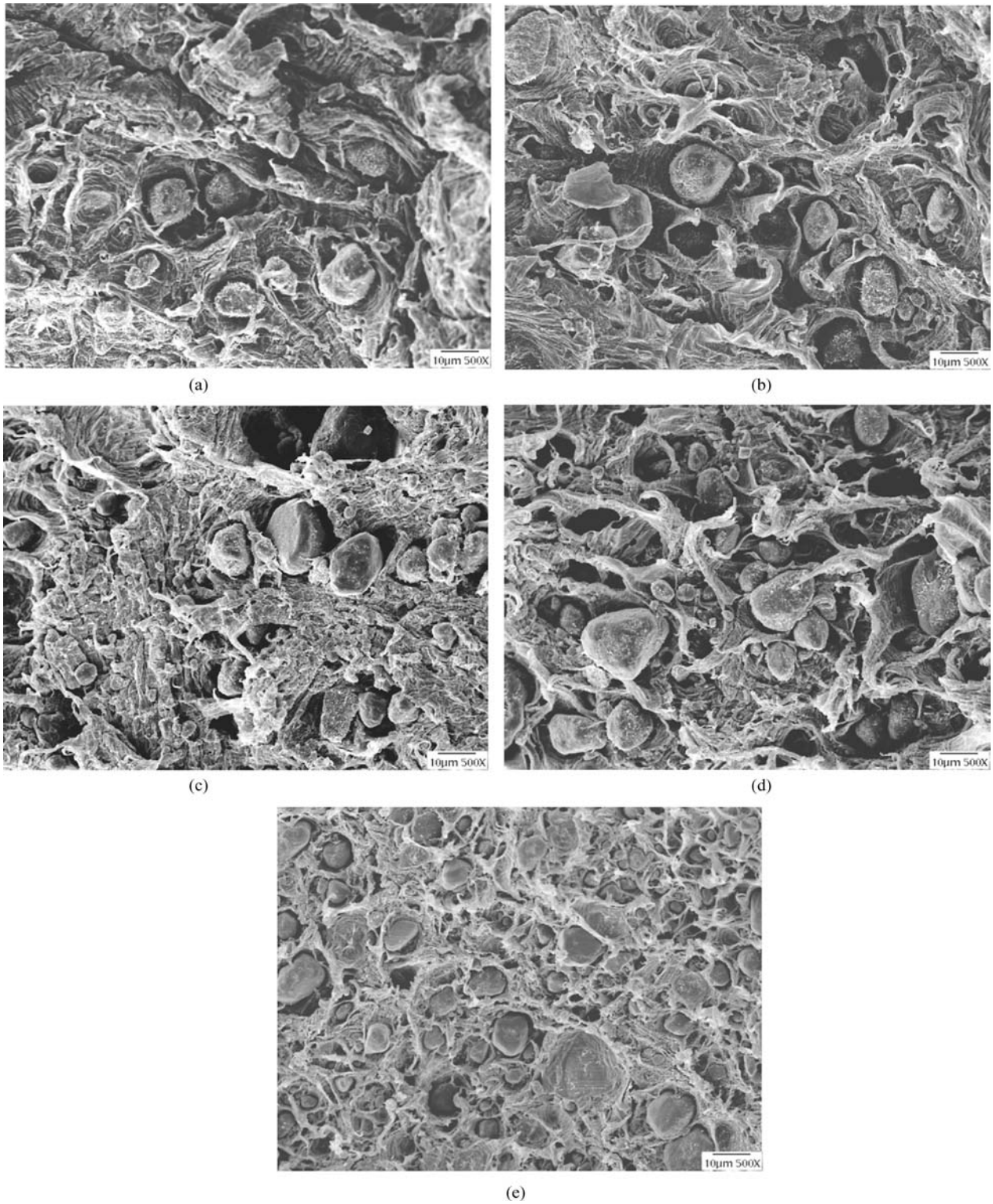

Figure 1 (a–e): SEM micrographs of HA/HDPE composite particles at a magnification of 500: (a) 10 wt%, (b) 20 wt%, (c) 30 wt%, (d) 40 wt%, and (e) 50 wt% hydroxyapatite.

HDPE matrix was reinforced with a blend of HDPE and HA. Fig. 3a–e shows SEM image of fractured surface at a magnification of 15000. It can be seen that HDPE fibrils attached to the HA particles make the reinforcement particles a HA-HDPE blend that reinforces the HDPE matrix. Presence of this fibrous morphology around the HA particles helps bind the reinforcement to the matrix, resulting in a better mechanical strength without the use of any chemical functionalization of the either the matrix or the reinforcement. It is worth mentioning that as the concentration of HA is increased in the composite the amount of fibrous HDPE attaching to the HA particles

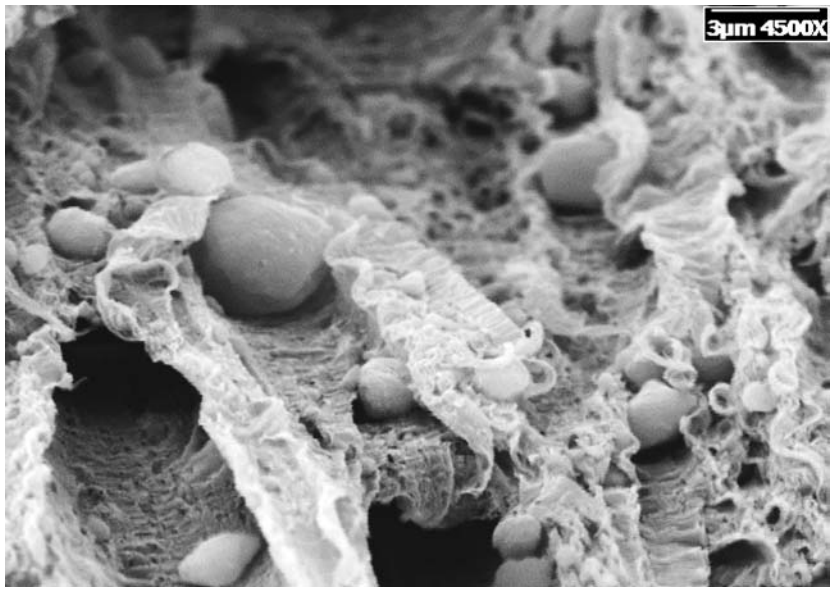

Figure 2 Fracture surface of HDPE-HA composite at a magnification of 4500.

reduces. Presence of these micro fibrils on the surface of HA results in better attachment of the reinforcement to the matrix and hence higher ductility to the composite.

3.2. Tension tests

Table II details the tensile test results. The tensile properties of HA-HDPE composites were measured under displacement rate of 25 mm/min while the load and extension were measured. From the change in gauge length of the sample, the percentage elongation at break was also calculated. In general, most of the samples exhibited localized yielding that is characteristic to semi-crystalline polymers. The stress-strain curves of the HA-HDPE composites are shown in Fig. 4. From the figure we can see that 10% HA composite has lower tensile strength but higher tensile strain compared to the composites having higher HA concentration. As the amount of HA is increased the individual HA-HDPE reinforcement particles have increasing amount of HA, resulting in increased thickness and stiffness but a significant decrease in ductility. The ductility is dependent on the number or amount of microfibrils that extend from the HA-HDPE reinforcement to the matrix. These micro anchoring sites are clearly evident in Fig. 3 which shows the number of these microfibrils decrease as the amount of HA increases.

3.3. XRD studies

XRD studies were carried out on hot rolled HDPE and hot rolled HDPE-HA composites with the objective to ensure that even after hot rolling, crystallinity of HDPE is conserved. Fig. 5 shows XRD pattern of a hot rolled HDPE sample. Presence of sharp peak at $2\theta = 24$ degrees matched well with the characteristic crystalline peak of HDPE as reported in literature [17, 18]. Powder samples of HA was examined for phase purity and structural changes on hot rolling, with a X-ray powder diffractometer using monochromatic Cu Ka radiation at 30 mA, 40 kV. The XRD peaks were indexed based on hexagonal crystal system of space group P63/m, with reference to JCPDS file no. 9-432. The results show all the characteristic peaks of HA. XRD spectrums of HA-HDPE composite were also analyzed. Fig. 6 shows XRD spectrum of the powdered HA-HDPE composites for 20%and 40% HA in HA-HDPE composites. Comparison of Figs 5 and 6 clearly showed that all the characteristic peak of HDPE and HA are present in the composites and processing by hot rolling preserved crystallinity of the HDPE and did not alter the structure of HA.

3.4. Differential Scanning Calorimetry (DSC)

DSC thermograms were obtained for all the composites. A standard heating rate of 5°C/ min, under N_2 atmosphere, was maintained up to melting temperatures for all samples. From the DSC spectra, the degree of crystallinity was calculated using the relationship

$$\chi = H_C/H \tag{1}$$

where H_c and H are the measured and the known values of heat of melting of HDPE, respectively. H was taken as 291.6 J/g, the value for 100% crystalline PE [19] and the experimental heat of melting values were calculated from the area under the exotherms. As the volume fraction of HA increased the crystallinity in the HDPE decreased as shown in Table 6.

3.5. FTIR studies

The IR spectra of pure components viz HDPE and HA as well as composites of variable composition of HA content from 10% to 50% are presented in the Figs 7–9, detailed analysis of components and composites are discussed below.III.

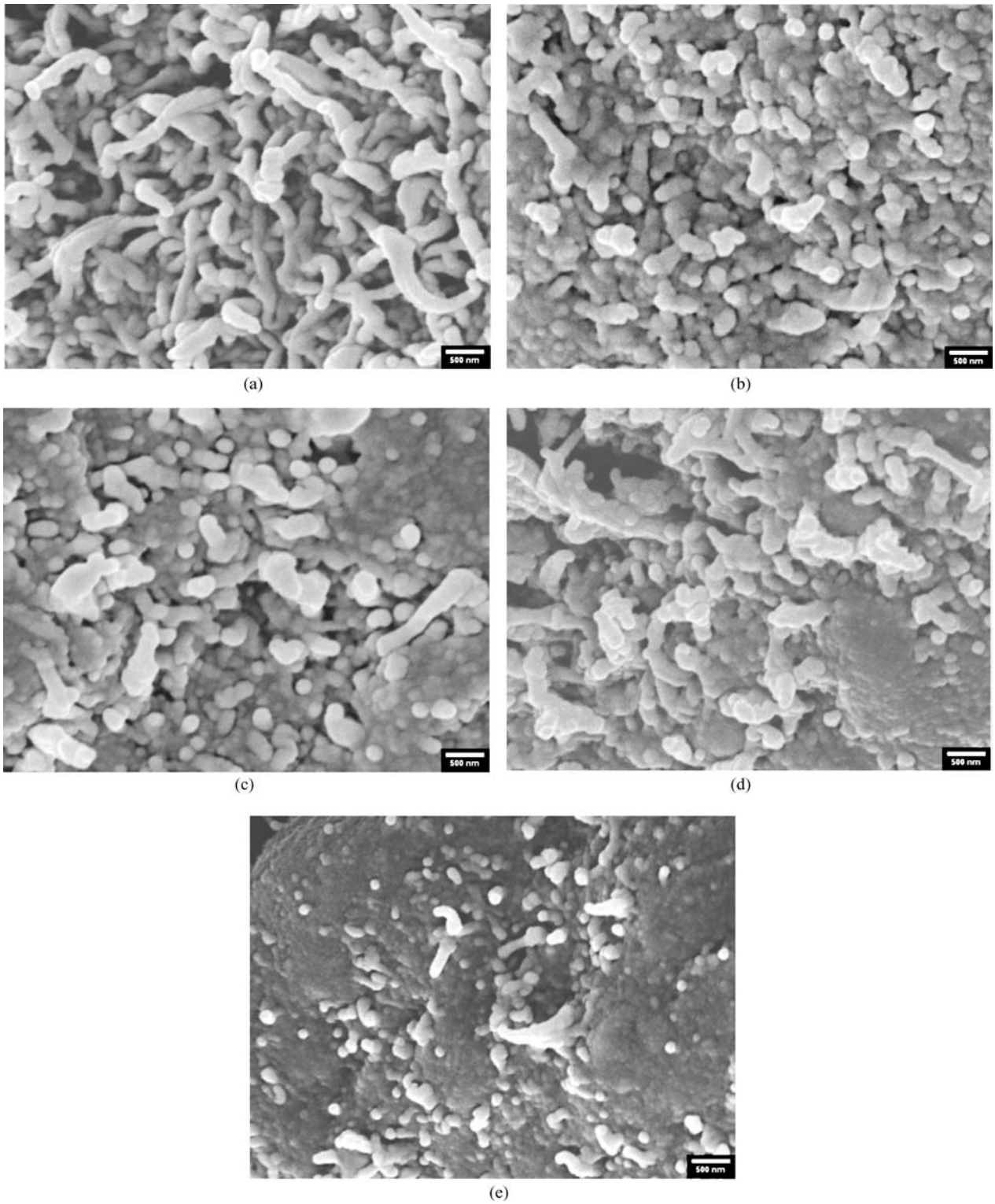

Figure 3 SEM micrographs of individual HA/HDPE composite particle at a magnification of 15000: (a) 10 wt%, (b) 20 wt%, (c) 30 wt%, (d) 40 wt%, and (e) 50 wt% hydroxyapatite.

3.5.1. FTIR of HA

HA being an inorganic compound ($Ca_5(PO_4)_3OH$) has a very simple IR spectrum. Most of the expected bands are observed typically in the lower region of the IR spectrum, corresponding to various vibrational modes of phosphate (PO_4) and hydroxyl groups in addition to their linkages with Ca. Peaks in the region 1050–1150 cm^{-1} and at 570–603 cm^{-1} are due to structural and P–O bonds of the phosphate group. The very weak bands around 3600 cm^{-1} and 1637 cm^{-1} are assigned to stretching and

TABLE II Young's modulus, tensile strength and% fracture strain of HDPE-HA composites under study. The data represents an average of 5 independent tests conducted for each condition

HA weight (%)	Young's modulus (MPa)	Tensile strength (MPa)	Fracture strain (%)
10	206.3 ± 31.9	20.2 ± 0.2	163.9 ± 51.5
20	324.6 ± 34.2	21.2 ± 0.4	63.5 ± 18.3
30	383.3 ± 31.9	21.4 ± 0.5	24.8 ± 4.8
40	396.3 ± 74.6	22.5 ± 0.4	17.5 ± 2.4
50	531.2 ± 75.6	24.3 ± 1.5	8.6 ± 1.1

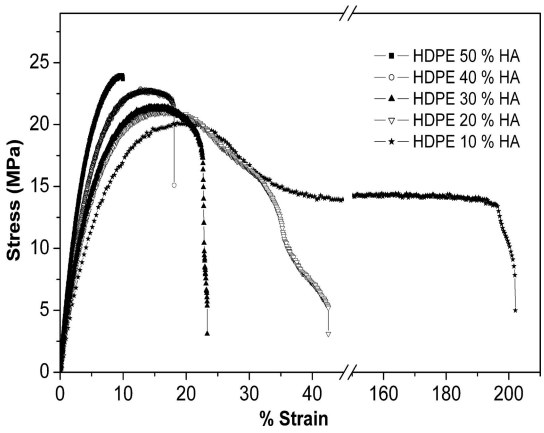

Figure 4 Representative stress-strain curves of the composites with different HA wt%. Only one typical plot for each condition is shown.

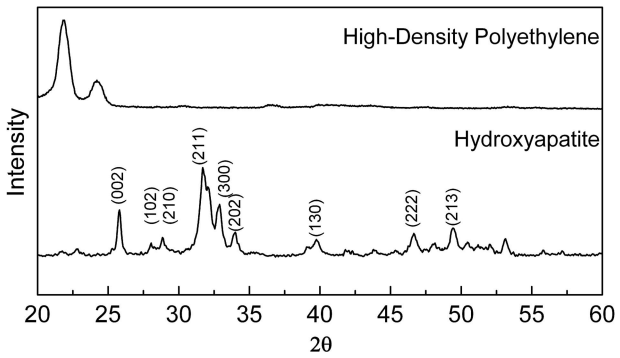

Figure 5 XRD spectrum of monolithic hot rolled HDPE and hydroxyapatite particles.

deformation modes of OH groups of HA respectively (not clearly visible in the spectrum due to the strong band of the PO_4 group).

3.5.2. FTIR of HDPE

Characteristic bands for HDPE are in good agreement with those reported in literature [20, 21]. Strong bands around 2920 cm^{-1} and 2850 cm^{-1} are of asymmetric and symmetric CH stretching of the methylene unit of polymer respectively. The doublet around 1468 cm^{-1} represents the C–H bending deformation and a weak band due to C–H symmetric deformation of terminal methyl group is present at 1377 cm^{-1} and the band at 722 cm^{-1} corresponds to the rocking deformation. Table IV enlists major absorptions of HDPE in the IR region and their assignment.

TABLE III Degree of crystallinity of HA-HDPE composites

Sample Number	% Hydroxyapatite	Crystallinity (%χ)
1	10%	57.71701
2	20%	48.14063
3	30%	41.02847
4	40%	34.19896
5	50%	27.62014

3.5.3. FTIR of HDPE-HA composite

Spectral analysis of the composites with different HA concentrations very clearly showed the formation of a very unique material as is evident from the typical HA characteristic bands, most of which tend to disappear/merge

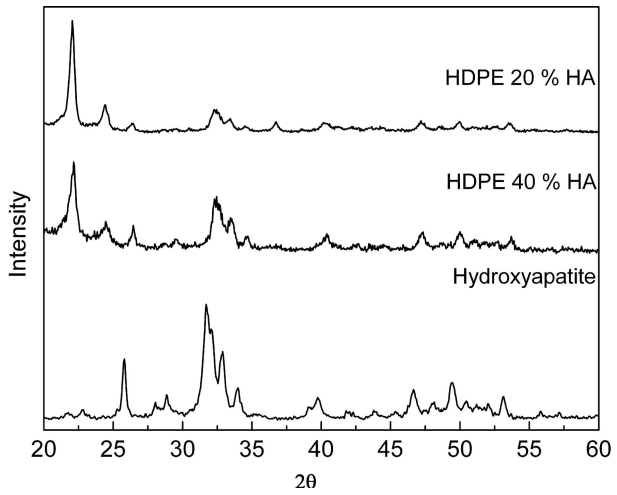

Figure 6 XRD spectrum of hot rolled HDPE-HA composite containing 20 and 40 wt% hydroxyapatite particles and HA particles by themselves.

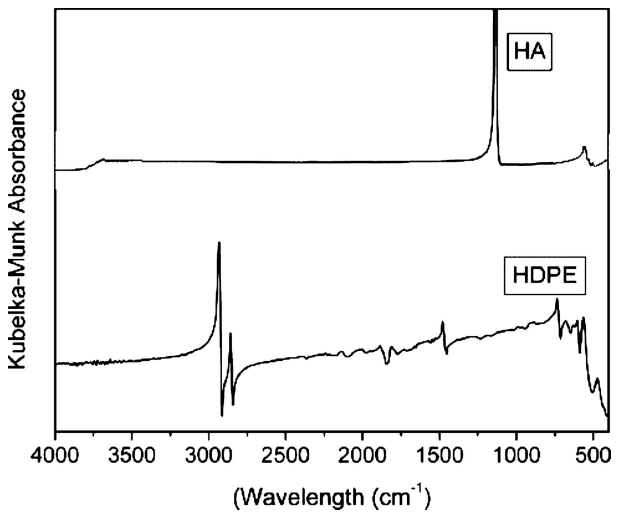

Figure 7 FTIR spectrum in diffuse reflectance mode of pure HA and HDPE.

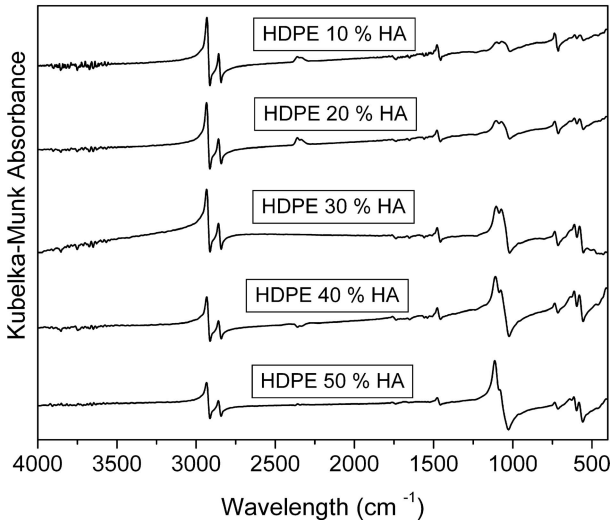

Figure 8 FTIR spectrums in diffuse reflectance mode of HA-HDPE composites.

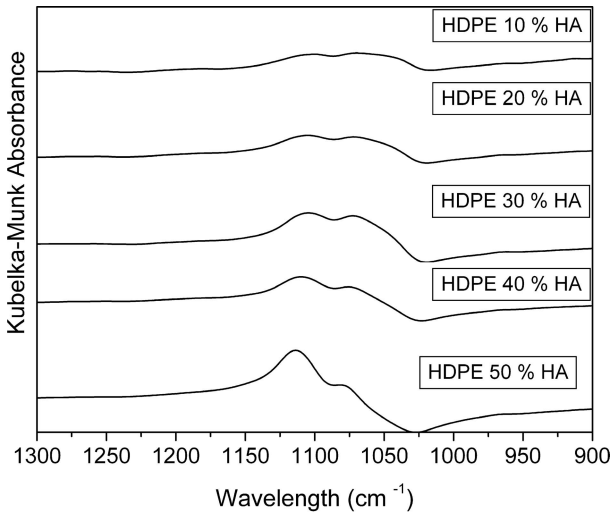

Figure 9 FTIR spectrums in diffuse reflectance mode of HA-HDPE composites in 900 cm^{-1} to 1300 cm^{-1} range.

or shift considerably with the typical bands of HDPE. In addition, deformation C–H bands around 1470 cm^{-1}, 722 cm^{-1} are considerably shifted from the original bands. Similarly the characteristic structural (tetrahedral) phosphate band (HA) around 1150 cm^{-1} is shifted to a clear doublet at 1110–1080 cm^{-1} in the composite. It is worth noting here that this doublet tends to change to a singlet with the increasing HA concentration where the second band at 1080 cm^{-1} becomes a weak shoulder in the composites with 40% and 50% of HA. This unique observation could possibly be due to some type of chemical interaction or induced-dipole attraction between HDPE and HA in the composites. This is further supported from the SEM images which shows the presence of HDPE microfibrils on HA surface and the amount of HA surface covered by HDPE microfibrils reduces with increasing concentration of HA. Recent study by J. Vandiver *et al.* [22] showed a net negative surface charge per unit area

TABLE IV Main absorption bands of HDPE in the IR region and their assignment

Band (cm^{-1})	Assignment	Intensity
2920	CH_2 Asymmetric stretching	Strong
2850	CH_2 Symmetric stretching	Strong
1468	CH Bending deformation	Medium
1377	CH_3 Symmetric deformation	Weak
722	rocking deformation	Medium

of HA particles vary from −0.0037 to −0.072 C/m^2 with an average of 0.02 C/m^2. Authors speculate this net negative charge may be responsible for the induced dipole attraction between the reinforcement and matrix.

4. Conclusions

The present study details a new method of synthesis of HDPE composites reinforced with hydroxyapatite. The composite synthesized had improved ductility and tensile strength without the addition of any coupling agent or surface treatment of HA particles. Tensile strength and Young's modulus of the composite increased with increasing concentration of reinforcement HA particles, while the fracture strain decreased.

Presence of micro fibrils on the surface of HA particles in SEM images, shifting of phosphate group peaks in FTIR spectrum suggests formation of an interfacial layer between the particles and matrix. This layer provides mechanical interlocking as well as chemical coupling between the two phases, resulting in higher ductility as well as higher tensile strengths of the composites.

Hot rolling is an effective method of composite synthesis. The matrix and the reinforcement particles were brought into intimate contact with each other by repeated pass between the rolls, and hence resulted in more uniformly distributed and well coupled reinforcement particles in HDPE matrix.

Acknowledgments

The authors graciously acknowledge the support form The Materials Science and Engineering program at University of Texas at Arlington. Use of FTIR equipment *n* the Department of Chemistry at the University of Texas at Arlington is gratefully acknowledged.

References

1. W. BONFIELD, M. D. GRYNPAS, A. E. TULLY, J. BOWMAN and J. ABRAM, *Biomater.* **2** (1981) 185.
2. J. ABRAM, J. BOWMAN, J. C. BEHIRI and W. BONFIELD, *Plast. Rub. Proc. Appl.* **4** (1984) 261.
3. W. BONFIELD, in "Engineering Applications of New Composites", edited by S. A. Paipetis and G. C. Papanicolaou (Omega Scientific, Oxford, 1988) p. 17.
4. G. P. EVANS, J. C. BEHIRI, J. D. CURREY and W. BONFIELD, *J. Mater. Sci. Mater. Med.* **1** (1990) 38.
5. F. J. GUILD and W. BONFIELD, *Biomaterials.* **14** (1993) 985.

6. M. WANG, D. PORTER and W. BONFIELD, *Br. Ceram. Trans.* **93** (1994) 91.
7. R. JOSEPH, W. J. MCGREGOR, M. T. MARTYN, K. E. TANNER and P. D. COATES, *Biomaterials.* **23** (2002) 4295.
8. RUI A. SOUSA, RUI L. REIS, ANTÓNIO M. CUNHA and MICHAEL J. BEVIS, *Comp. Sci. Tech.* **63** (2003) 389.
9. M. WANG and W. BONFIELD, *Biomaterials.* **22** (2001) 1311.
10. W. SUCHANEK and M. YOAHIMURA, *J. Mater. Res.* **13** (1998) 94.
11. L. L. HENCH, Bioceramics. *J. Am. Ceram. Soc.* **81** (1998) 1705.
12. V. A. DUBOK, Bioceramics– yesterday, today, tomorrow. *Powder Metall. Met. Ceram.* **39** (2000) 381.
13. P. DUCHEYNE and Q. QIU, *Biomaterials.* **20** (1999) 2287.
14. J. D. DE BRUIJN, C. P. A. T. KLEIN, K. DE GROOT and V. C. A. VAN BLITTERSWIJK, *J. Biomed. Mater. Res.* **26** (1992) 1365.
15. C. D. HAN, C. SANDFORD and H. J. YOO, *Polym. Engng. Sci.* **18** (1979) 849.
16. W. Y. CHIANG and W. D. YANG, *J. Appl. Polym. Sci.* **35** (1988) 807.
17. S. O. HAN, D. W. LEE and O. H. HAN, *Poly. Degrad. Stab.* **63** (1999) 237.
18. A. MARKIEWICZ, R. E. MAYESB MOUBARAKI and K. S. MURRAY, *Mat. Res. Bull.* **29** (1994) 393.
19. J. AKHAVAU and P. J. HENDRA, *Polymer.* **26** (1985) 865.
20. J. V. GULMINE, P. R. JANISSEK, H. M. HEISE and L. AKCELRUD, *Poly. Test.*. **21** (2002) 557.
21. G. A. GEORGE, M. CELINA, A. M. VASSALLO and P. A. COLE-CLARKE, *Polym. Degrad Stab* **48** (1995) 199.
22. J. VANDIVER, D. DEAN, N. PATEL, W. BONFIELD and C. ORTIZ, *Biomaterials* **26** (2005) 271.

Received x x
and accepted 11 July 2005